New Metal Chalcogenides Found in $Mn_{N-1}(Gd_{2-x}In_x)S_{N+2}$ (N = 3, 4, 5): Syntheses, Structures, and Magnetic Properties

I. C. Liang,[a] C. Y. Weng,[a] C. Huang,[a] C. K. Chang,[b] H. S. Sheu,[b] J. G. Lin,[c] and K. F. Hsu[a,*]

[a]*Department of Chemistry, National Cheng Kung University, Tainan 701, Taiwan*
[b]*National Synchrotron Radiation Research Center, Hsinchu 300, Taiwan*
[c]*Center for Condensed Matter Sciences, National Taiwan University, Taipei 106, Taiwan*

Table S1. Atomic coordinates, thermal parameters (Å^2) and occupancies for **1**, **1a**, **2**, and **3**.

Table S2. Selected bond distances (Å) for **1** and **1a**.

Table S3. Selected bond distances (Å) for **2** and **3**.

Figure S1. (a) The SEM image of a tiny Gd_2S_3 crystal grew and embedded on the surface of large columnar crystal **3**. (b) An enlargement image of the selected area (blue circle) in (a).

Figure S2. The powder X-ray diffraction (PXRD) pattern of **1** and **1a** was measured by a Bruker AXS D2 phaser equipped with a Cu K_α tube (λ = 1.5406 Å) and a one-dimensional LYNXEYE detector.

Figure S3 The measured (blue) and simulated (red) PXRD patterns of **1**. The inset plot is an enlarged simulated pattern of **1** in 2θ angles of 14–16 degree.

Figure S4 The measured (blue) and simulated (red) PXRD patterns of **3**. The blue labels of (hkl) denote the diffraction peaks promoted by a high resolution X-ray radiation (λ = 0.7749 Å). The purple labels of (hkl) denote some simulated diffraction peaks of **3**. The black stars denote the impurity.

Figure S5. The measured (blue) PXRD patterns of **3** and simulated (green) PXRD pattern of La_2S_3-type Gd_2S_3. The black stars denote the impurity.

Figure S6. The EDS measurements of (a) **1**, (b) **2** and (c) **3**.

Table S1. Atomic coordinates, thermal parameters (Å^2) and occupancies for **1**, **1a**, **2**, and **3**.

Atom	*x/a*	*y/b*	*z/c*	U_{eq}[a]	occ.
			1		
Gd(1)	0	0.4711(1)	1/4	0.012(1)	1
Mn(2)/In(2')	0	0.7275(1)	0.3951(1)	0.013(1)	0.858(3)/0.142
Mn(3)/In(3')	1/2	1/2	1/2	0.011(1)	0.234(5)/0.766
S(1)	1/2	0.3140(1)	1/4	0.010(1)	1
S(2)	1/2	0.5859(1)	0.3550(1)	0.009(1)	1
S(3)	1/2	0.8614(1)	0.4476(1)	0.012(1)	1
			1a		
Gd(1)	0	0.4727(1)	1/4	0.016(1)	1
Mn(2)/Gd(2')	0	0.7276(1)	0.3963(1)	0.015(1)	0.765(2)/0.235
Mn(3)/In(3')	1/2	1/2	1/2	0.015(1)	0.514(5)/0.486
S(1)	1/2	0.3157(1)	1/4	0.015(1)	1
S(2)	1/2	0.5847(1)	0.3553(1)	0.012(1)	1
S(3)	1/2	0.8631(1)	0.4477(1)	0.017(1)	1
			2		
Gd(1)	0	0.3422(1)	1/4	0.015(1)	1
Mn(2)/Gd(2')	1/2	0.0936(1)	0.3721(1)	0.013(1)	0.556(2)/0.444
Mn(3)/Gd(3')	1/2	0.6389(1)	0.5414(1)	0.014(1)	0.947(2)/0.053
S(1)	1/2	0.1843(1)	1/4	0.014(1)	1
S(2)	1/2	0.4473(1)	0.3380(1)	0.011(1)	1
S(3)	1/2	0.7278(1)	0.4176(1)	0.014(1)	1
S(4)	0	1/2	1/2	0.013(1)	1
			3		
Gd(1)	0	0.2940(1)	3/4	0.014(1)	1
Mn(2)/Gd(2')	0	0.0426(1)	0.6452(1)	0.012(1)	0.578(2)/0.422
Mn(3)/Gd(3')	1/2	0.2749(1)	0.5715(1)	0.013(1)	0.961(2)/0.039
Mn(4)/Gd(4')	0	1/2	1/2	0.014(1)	0.929(2)/0.071
S(1)	1/2	0.4525(1)	3/4	0.013(1)	1
S(2)	1/2	0.1888(1)	0.6744(1)	0.010(1)	1
S(3)	0	0.4087(1)	0.6061(1)	0.013(1)	1
S(4)	0	0.1375(1)	0.5344(1)	0.011(1)	1

[a] U_{eq} is defined as one third of the trace of the orthogonalized U_{ij} tensor.

Table S2. Selected bond distances (Å) for **1** and **1a**.

	1		**1a**
Gd(1)–S(1)[a]	2.718 (1)	Gd(1)–S(1)[a]	2.723(2)
Gd(1)–S(1)	2.718(1)	Gd(1)–S(1)	2.723(2)
Gd(1)–S(2)	2.875(1)	Gd(1)–S(2)	2.870 (1)
Gd(1)–S(2)[b]	2.875(1)	Gd(1)–S(2)[b]	2.870(1)
Gd(1)–S(2)[c]	2.875(1)	Gd(1)–S(2)[c]	2.870(1)
Gd(1)–S(2)[a]	2.875(1)	Gd(1)–S(2)[a]	2.870(1)
Gd(1)–$S_{Ave.}$	**2.823(1)**	**Gd(1)–$S_{Ave.}$**	**2.821(1)**
M(2)–S(1)[e]	2.491(1)	M(2)–S(1)[e]	2.535(1)
M(2)–S(3)	2.649(1)	M(2)–S(3)	2.662(1)
M(2)–S(3)[a]	2.649(1)	M(2)–S(3)[a]	2.662(1)
M(2)–S(2)[a]	2.657(1)	M(2)–S(2)[a]	2.678(1)
M(2)–S(2)	2.657(1)	M(2)–S(2)	2.678(1)
M(2)–S(3)[f]	2.674(2)	M(2)–S(3)[f]	2.685(2)
M(2)–$S_{Ave.}$	**2.630(1)**	**M(2)–$S_{Ave.}$**	**2.650(1)**
M(3)–S(2)[e]	2.486(2)	M(3)–S(2)[f]	2.494(1)
M(3)–S(2)[f]	2.486(2)	M(3)–S(2)[e]	2.494(1)
M(3)–S(3)[g]	2.684(1)	M(3)–S(3)[g]	2.678(1)
M(3)–S(3)[a]	2.684(1)	M(3)–S(3)[a]	2.678(1)
M(3)–S(3)[h]	2.684(1)	M(3)–S(3)[h]	2.678(1)
M(3)–S(3)	2.684(1)	M(3)–S(3)	2.678(1)
M(3)–$S_{Ave.}$	**2.618(1)**	**M(3)–$S_{Ave.}$**	**2.617(1)**

Symmetry code: [a]x–1, y, z; [b]x–1, y, –z+1/2; [c]x, y, –z+1/2; [d]x+1, y, z; [e]x–1/2, y+1/2, z; [f]–x+1/2, –y+3/2, –z+1; [g]–x+1, –y+2, –z+1; [h]–x, –y+2, –z+1; [i]x+1/2, y–1/2, –z+1/2; [j]x+1/2, y–1/2, z.

Table S3. Selected bond distances (Å) for **2** and **3**.

2		**3**	
Gd(1)-S(1)[a]	2.733(1)	Gd(1)-S(1)	2.731(1)
Gd(1)-S(1)	2.733(1)	Gd(1)-S(1)[a]	2.731(1)
Gd(1)-S(2)	2.850(1)	Gd(1)-S(2)[a]	2.848(1)
Gd(1)-S(2)[b]	2.850(1)	Gd(1)-S(2)[o]	2.848(1)
Gd(1)-S(2)[c]	2.850(1)	Gd(1)-S(2)[p]	2.848(1)
Gd(1)-S(2)[a]	2.850(1)	Gd(1)-S(2)	2.848(1)
Gd(1)–$S_{Ave.}$	**2.811(1)**	**Gd(1)–$S_{Ave.}$**	**2.809(1)**
M(2)-S(1)	2.595(1)	M(2)-S(1)[h]	2.593(1)
M(2)-S(3)[g]	2.673(1)	M(2)-S(3)[h]	2.665(1)
M(2)-S(3)[h]	2.673(1)	M(2)-S(3)[g]	2.665(1)
M(2)-S(2)[h]	2.709(1)	M(2)-S(2)	2.702(1)
M(2)-S(2)[g]	2.709(1)	M(2)-S(2)[a]	2.702(1)
M(2)-S(4)[g]	2.710(1)	M(2)-S(4)	2.737(1)
M(2)–$S_{Ave.}$	**2.678(1)**	**M(2)–$S_{Ave.}$**	**2.677(1)**
M(3)-S(2)[i]	2.547(1)	M(3)-S(2)	2.531 (1)
M(3)-S(3)	2.613(1)	M(3)-S(4)[n]	2.602(1)
M(3)-S(3)[j]	2.638(1)	M(3)-S(3)[d]	2.632(1)
M(3)-S(3)[k]	2.638(1)	M(3)-S(3)	2.632(1)
M(3)-S(4)	2.685(1)	M(3)-S(4)	2.678(1)
M(3)-S(4)[d]	2.685(1)	M(3)-S(4)[d]	2.678(1)
M(3)–$S_{Ave.}$	**2.634(1)**	**M(3)–$S_{Ave.}$**	**2.626(1)**
		M(4)-S(3)[m]	2.624(1)
		M(4)-S(3)	2.624(1)
		M(4)-S(4)[q]	2.660(1)
		M(4)-S(4)[l]	2.660(1)
		M(4)-S(4)[n]	2.660(1)
		M(4)-S(4)[e]	2.660(1)
		M(4)–$S_{Ave.}$	**2.648(1)**

Symmetry code: [a]x–1, y, z; [b]x–1, y, –z+1/2; [c]x, y, –z+1/2; [d]x+1, y, z; [e]x–1/2, y+1/2, z; [f]x–1/2, y+1/2, –z+1/2; [g]x+1/2, y–1/2, z; [h]x–1/2, y–1/2, z; [i]–x+1, –y+1, –z+1; [j]–x+3/2, –y+3/2, –z+1; [k]–x+1/2, –y+3/2, –z+1; [l]x+1/2, y+1/2, z; [m]–x, –y+1, –z+1; [n]–x+1/2, –y+1/2, –z+1; [o]x, y, –z+3/2; [p]x–1, y, –z+3/2; [q]–x–1/2, –y+1/2, –z+1; [r]x+1/2, y+1/2, –z+3/2.

(a)

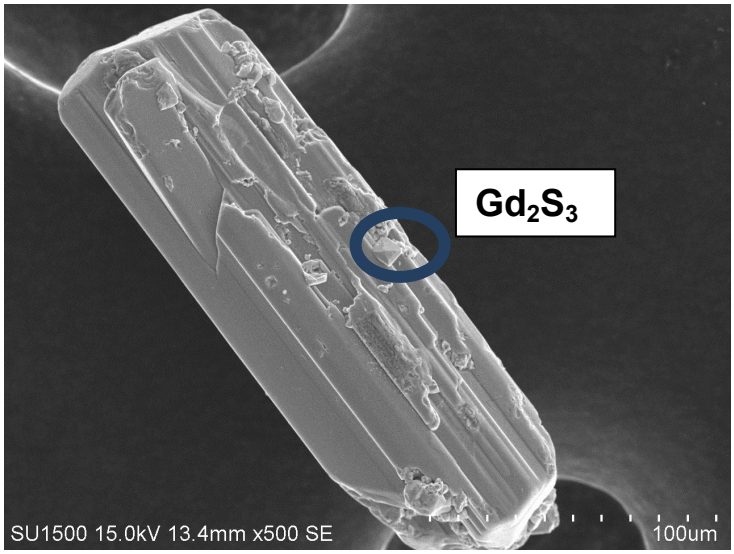

(b)

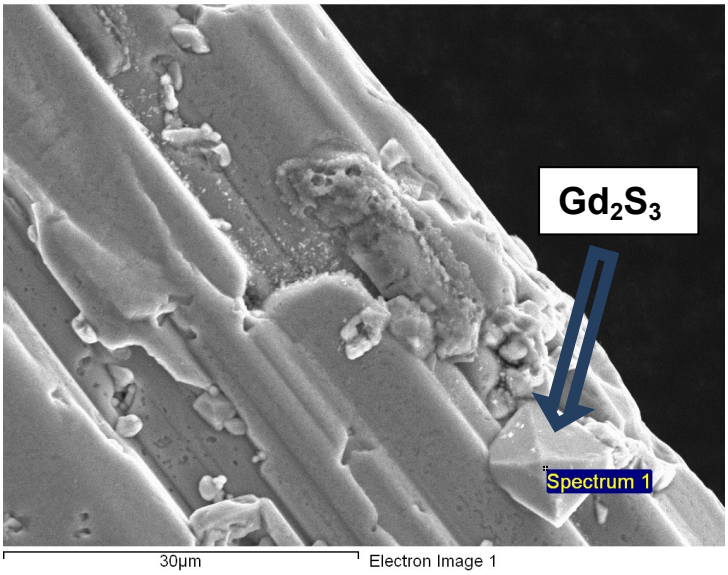

Figure S1. (a) The SEM image of a tiny Gd_2S_3 crystal grew and embedded on the surface of large columnar crystal **3**. (b) An enlargement image of the selected area (blue circle) in (a).

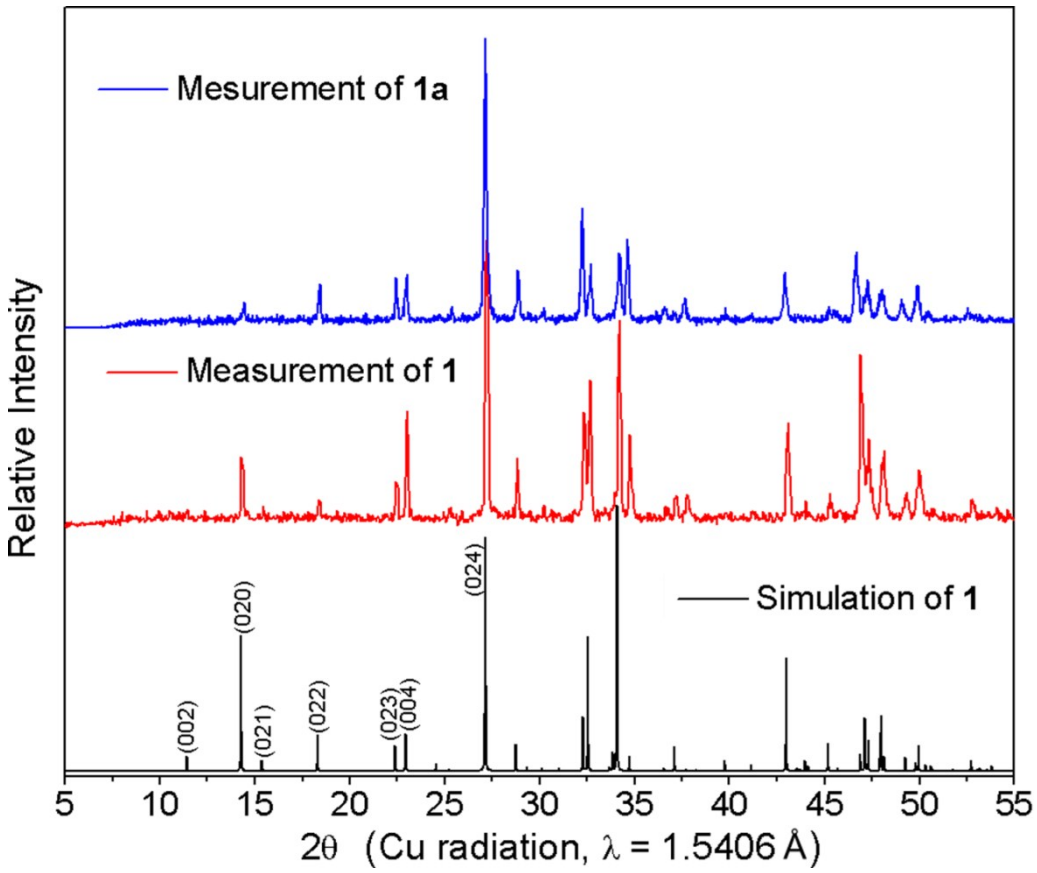

Figure S2. The powder X-ray diffraction (PXRD) pattern of **1** and **1a** was measured by a Bruker AXS D2 phaser equipped with a Cu K_α tube (λ = 1.5406 Å) and a one-dimensional LYNXEYE detector.

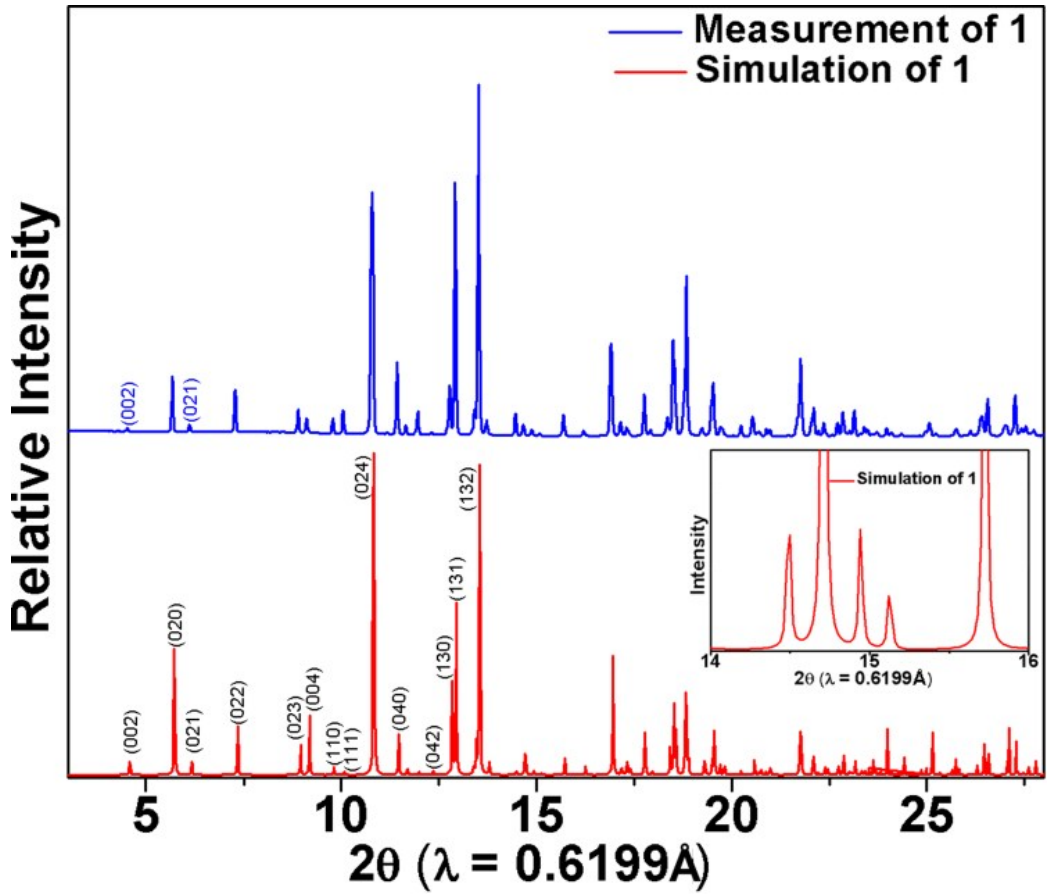

Figure S3. The measured (blue) and simulated (red) PXRD patterns of **1**. The inset plot is an enlarged simulated pattern of 1 in 2θ angles of 14–16 degree.

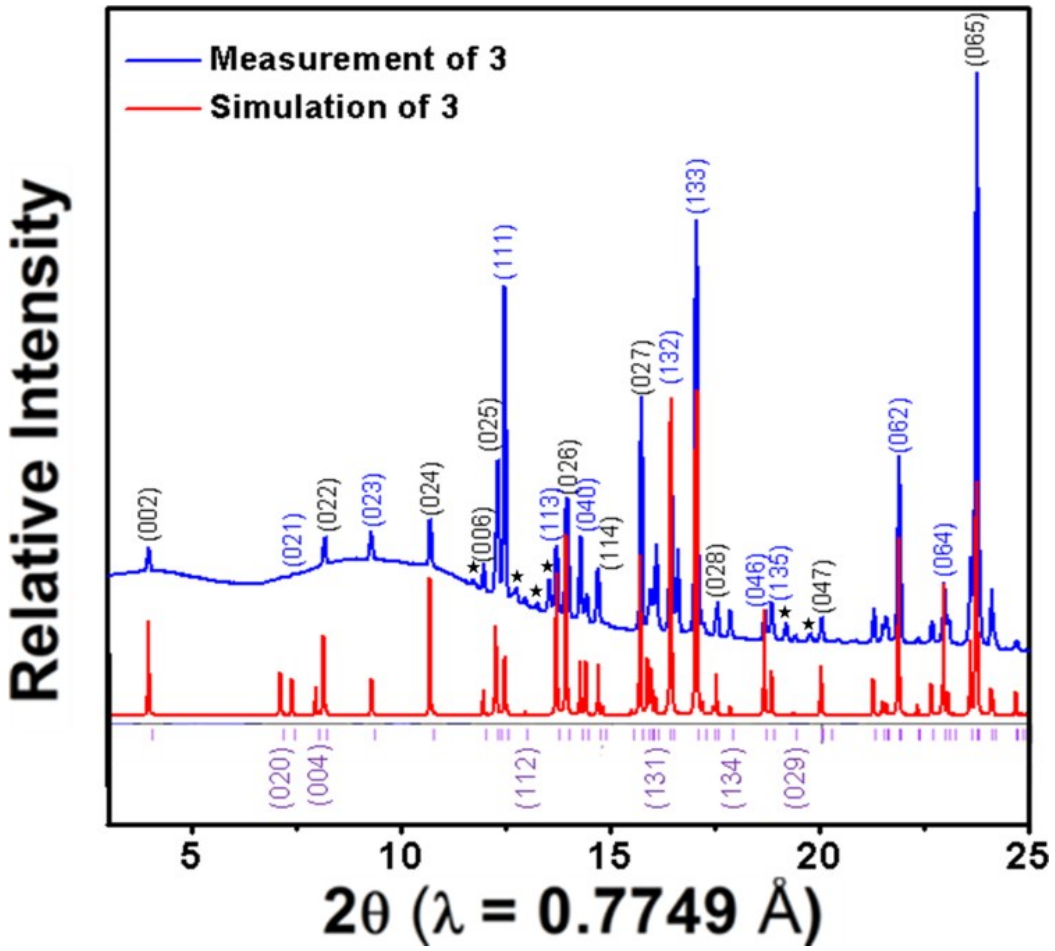

Figure S4. The measured (blue) and simulated (red) PXRD patterns of **3**. The blue labels of (hkl) denote the diffraction peaks promoted by a high resolution X-ray radiation (λ = 0.7749 Å). The purple labels of (hkl) denote some simulated diffraction peaks of **3**. The black stars denote the impurity.

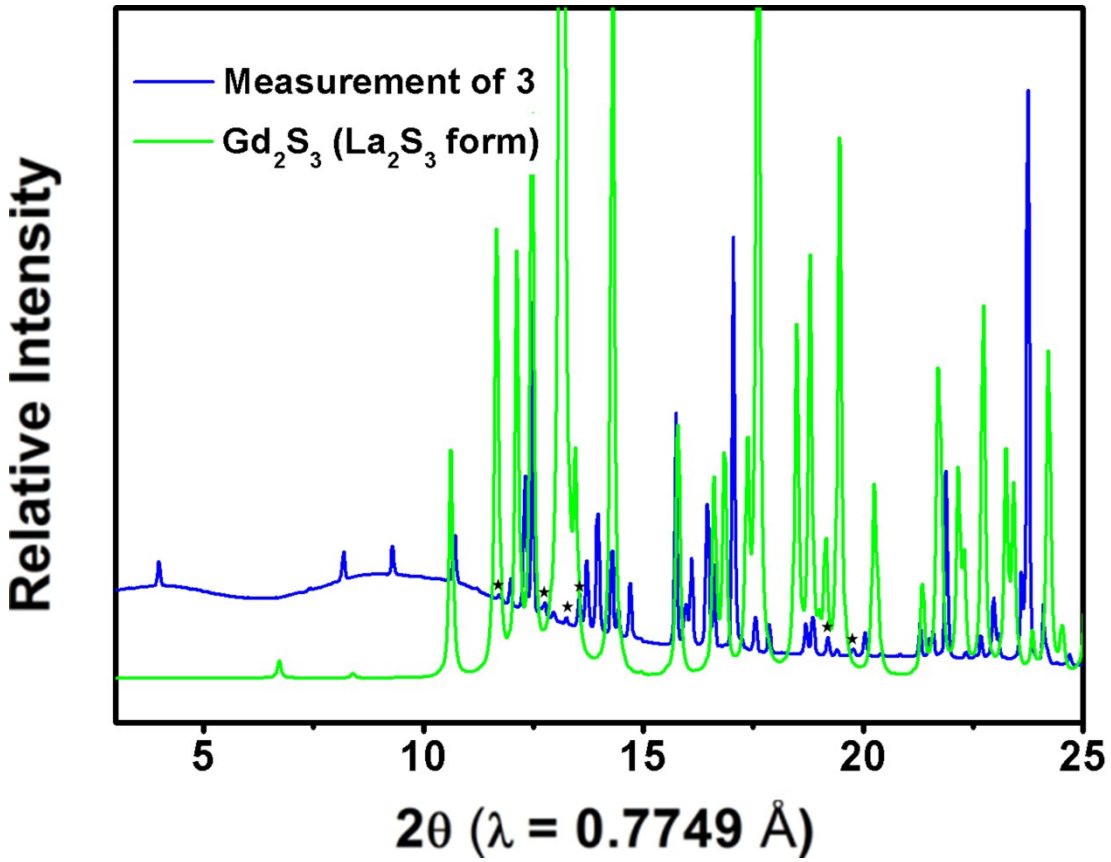

Figure S5. The measured (blue) PXRD patterns of **3** and simulated (green) PXRD pattern of La_2S_3-type Gd_2S_3. The black stars denote the impurity.

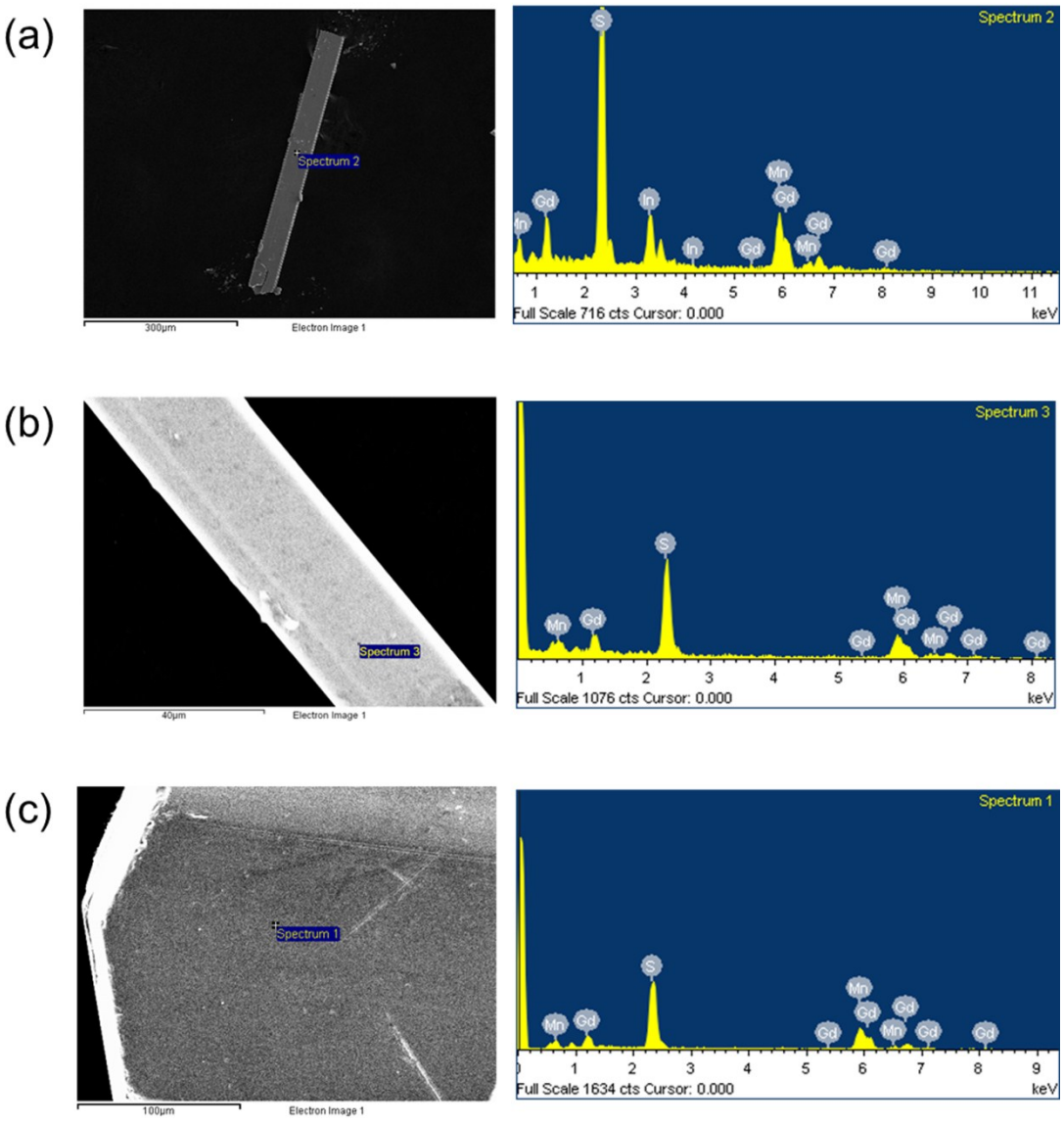

Figure S6. The EDS measurements of (a) **1**, (b) **2** and (c) **3**.